Simultaneous influence of additive and multiplicative noise on stationary dissipative solitons

Carlos Cartes,[1] Orazio Descalzi,[1,2,*] and Helmut R. Brand[2]

[1]*Complex Systems Group, Facultad de Ingeniería y Ciencias Aplicadas, Universidad de los Andes, Av. Mons. Álvaro del Portillo 12.455, Las Condes, Santiago, Chile*

[2]*Department of Physics, University of Bayreuth, 95440 Bayreuth, Germany*

(Received 25 January 2019; revised manuscript received 18 May 2019; published 25 July 2019)

We investigate the simultaneous influence of spatially homogeneous multiplicative noise as well as of spatially δ-correlated additive noise on the formation of localized patterns in the framework of the cubic-quintic complex Ginzburg-Landau equation. Depending on the ratio between the strength of additive and multiplicative noise we find a number of distinctly different types of behavior including explosions, collapse, filling in, and spatio-temporal disorder as well as intermittent behavior of all types listed. Techniques used to analyze the results include snapshots, x-t plots and plots of the spatially and temporally averaged amplitude as a function of the strength of multiplicative noise while keeping the strength of additive noise fixed. Typically 50 realizations are used for averaging to obtain the corresponding data points in these diagrams. For the widths of these distribution as a function of additive noise we obtain a linear decrease in the limit of fairly large, but fixed values of the multiplicative noise. To summarize our findings concisely we show three-dimensional plots of the mean pattern amplitude and the generalized susceptibility as a function of the strengths of additive and multiplicative noise. We critically compare the results of our investigations with those obtained in the two limiting cases of purely additive and of purely multiplicative noise.

DOI: 10.1103/PhysRevE.100.012214

I. INTRODUCTION

In driven, out-of-equilibrium macroscopic systems, noise may play a constructive or destructive role. For instance, biological systems can evolve in a way that they can take advantage of natural fluctuations. There the influence of noise ranges from the development of multicellular mechanisms to population dynamics [1,2]. Escape of a system from a metastable state is another example of the constructive role of fluctuations. In electronics unwanted disturbances reflect a nonconstructive role of noise. Sources of noise can be internal, like thermal noise, which is unavoidable at nonzero temperature, or external, like a fluctuating applied electric voltage, a fluctuating temperature gradient, or input flux of reactants. Systems involving rapid fluctuations can be modeled by Langevin equations, that is, stochastic differential equations for field variables [3–5]. Internal noise, typically, appears as an additive contribution [6], whereas external noise becomes multiplicative or both [7,8]. When the noise is only additive, the maxima of the stationary probability distribution correspond to the deterministic steady state of the system. Experimentally, in a surface reaction, namely, the catalytic oxidation of CO on Pd(111), probability distributions due to intrinsic noise have been measured [9]. Different is the scenario in the presence of multiplicative noise where systems might exhibit noise-induced transitions. Indeed, experiments have shown that a parametric oscillator exhibits an oscillatory to nonoscillatory transition controlled by the noise intensity [10]. The photon statistics of a dye laser has been obtained experimentally [11] and compared with the exact solution of a laser model with fluctuating pump parameter [12]. In the Brusselator, also subject to multiplicative noise but colored, postponement of the supercritical Hopf bifurcation has been studied, both theoretically [13] and experimentally [14]. The response of the stochastic subcritical Hopf-like model is presented in Ref. [15].

So far, the above discussion has not involved spatial degrees of freedom. Out-of-equilibrium, spatially extended, and stochastic systems are the framework of this article. The catalytic CO oxidation on single-crystal surfaces offers an excellent opportunity to study the influence of noise. On the one hand, in a mean field approach, the reaction-diffusion equations for certain metals are well established allowing the numerical study since all kinetic coefficients are known experimentally. On the other hand, experiments under UHV conditions allow one to vary the temperature and the CO fraction in the total input gas flux. Thus, the external noise imposed on the system can become purely multiplicative [16] or simultaneously additive and multiplicative [17].

Spatiotemporal patterns due to noise-induced phase transitions, including nucleation and growth of islands, have been studied for the CO oxidation reaction on Ir(111) [18–20]. We use throughout this paper the term noise-induced phase transitions in the spirit of Ref. [21] for spatially extended systems. The constructive role of noise becomes clear in an excitable photosensitive BZ medium, which may rectify external fluctuations into chemical waves [22], and by the catalytic CO oxidation on Pt(110), where global noise can suppress chemical turbulence [23]. A theoretical overview of the mechanisms through which noise can induce, enhance, or sustain ordered behavior is presented in Ref. [21].

*Corresponding author: odescalzi@miuandes.cl

Rayleigh-Bénard convection is a paradigm within the field of pattern-forming systems. Symmetry-breaking instabilities lead to patterns (nonequilibrium dissipative structures [24]). Initial stages of pattern formation have been experimentally measured revealing the importance of stochastic effects [25,26]. Electro-convection in nematic liquid crystal is another example of a pattern-forming system. In a thin layer fluctuations below the onset of electro-convection were measured. Results indicate that fluctuations are due to thermal noise [27]. In addition, experimentally it has been found that spatially homogeneous multiplicative (parametric) noise can shift or suppress the onset of pattern formation [28,29].

From a theoretical point of view, near an instability, it is possible to reduce the dynamics of the system to simpler equations (compared to the full system) that have a universal form. These envelope equations (including nonlinearities) account for the modulation (in space and time) of the linear unstable modes close to instabilities and reflect the underlying symmetries of the system [30–32]. The complex cubic-quintic Ginzburg-Landau equation (CQGLE) is an envelope equation derived, in the context of convective binary fluids, near the onset of a weakly inverted bifurcation to traveling waves [33]. Owing to the coexistence of the zero and one homogeneous state this equation shows, inside this bistable region, stable pulses as solutions, provided the feedback stabilization mechanism occurs [34]. In binary fluid convection, when the conductive state coexists with the convective state, localized regions of traveling waves have been reported [35,36]. These nonequilibrium localized structures are stabilized by a complex balance between nonlinearity and dispersion as well as between energy input and dissipation, extending the concept of conservative soliton to a dissipative soliton (DS) [37]. The examples of DSs transcend the convection systems. Indeed, these include nonlinear optics [38–41], granular media [42], surface reactions [43], and biology [44]. In addition to stationary pulses [34,45,46], the complex CQGLE exhibits periodic, quasiperiodic, and chaotic solutions [47]. Furthermore, asymmetric moving pulses, pulsating localized structures, and a period-doubling sequence have been reported [48,49].

One striking form of DS is that obtained in a Kerr lens mode-locked Ti:sapphire laser [50], and in an all-normal-dispersion Yb-doped mode-locked fiber laser [51], which had been predicted theoretically in the complex CQGLE in an optical framework, for anomalous linear dispersion [52], namely, exploding DSs. Because of spatiotemporal chaos exhibited by the observed explosions, they become similar but not identical, which leads to a distribution of times between explosions.

The influence of noise on counterpropagating and single DSs has been investigated, in particular, in the framework of the complex CQGLE. On the one hand, it was shown that weak additive noise can induce partial annihilation of colliding pulses [53]. On the other hand, for single pulses (either stationary or oscillatory) it was demonstrated that a small amount of additive noise can induce explosions [54], and for large additive noise the interaction of localization and noise can lead to noisy localized structures [55]. Recently, we have investigated the influence of spatially homogeneous multiplicative noise on pulses. We found that for large enough noise the formation of stationary, oscillatory and exploding pulses is suppressed [56].

Here we study the question of stationary dissipative solitons in the framework of the complex CQGLE under the simultaneous influence of spatially homogeneous multiplicative noise as well as of spatially δ-correlated additive noise. As a function of the relative strength between additive and multiplicative noise we find meandering exploding dissipative solitons, collapse, spatio-temporal disorder behavior, and filling in as possible outcomes as well as intermittent behavior of these various outcomes. To summarize the results obtained in a concise fashion we present three-dimensional plots of the mean pattern amplitude and its standard deviation as a function of the strength of additive and multiplicative noise, respectively.

The paper is organized as follows. In Sec. II we describe the model and the techniques used to analyze the results. In Sec. III we present the results and their discussion. In Sec. IV a comparison of the results of the present paper to the cases of purely additive and purely multiplicative noise is given. In Sec. V we provide a general picture using noise-induced phase transitions, and we end with conclusion and perspective.

II. THE MODEL

Of interest in our study are driven systems, which can support dissipative solitons in contrast to systems in or near equilibrium. Frequently the associated experimental investigations are performed close to an instability such as the onset of thermal convection in simple fluids or electroconvection in nematic liquid crystals. Since our goal is to encourage more systematic experimental work on the influence of additive and multiplicative noise on DSs, we investigate here a minimal model satisfying these requirements, namely, the CQGLE with additive and multiplicative noise

$$\begin{aligned}\partial_t A = \; & \mu A + (\beta_r + \mathrm{i}\beta_i)|A|^2 A + (\gamma_r + \mathrm{i}\gamma_i)|A|^4 A \\ & + (D_r + \mathrm{i}D_i)\partial_{xx} A + A\,\eta_m\,\xi(t) + \eta_a\,\zeta(x,t), \quad (1)\end{aligned}$$

where $A(x,t)$ is a complex field, β_r is positive, and γ_r is negative in order to guarantee that the bifurcation is subcritical but saturates to quintic order. The stochastic force $\zeta(x,t)$ denotes white noise with the properties $\langle\zeta\rangle = 0$, $\langle\zeta(x,t)\,\zeta(x',t')\rangle = 0$ and $\langle\zeta(x,t)\,\zeta^*(x',t')\rangle = 2\delta(x-x')\delta(t-t')$, where ζ^* denotes the complex conjugate of ζ. The stochastic force $\xi(t)$ denotes white noise with the properties $\langle\xi\rangle = 0$, and $\langle\xi(t)\,\xi(t')\rangle = \delta(t-t')$. That means we consider (a) additive noise, which is δ-correlated in time and space, and (b) multiplicative noise, which is real and homogeneous in space. In addition, we assume that there are no cross-correlations between additive and multiplicative noise.

Multiplicative noise is experimentally frequently achieved by superposing externally and spatially homogeneously noise on the driving force. This means one superposes spatially homogeneous noise on the driving voltage in electroconvection [29] in nematic liquid crystals, on the applied temperature gradient in thermal convection, or on the mean temperature for surface reactions [16]. Spatially homogeneous multiplicative noise also arises in certain optical systems such as the dye laser [11,12]. Applying spatially homogeneous noise on the

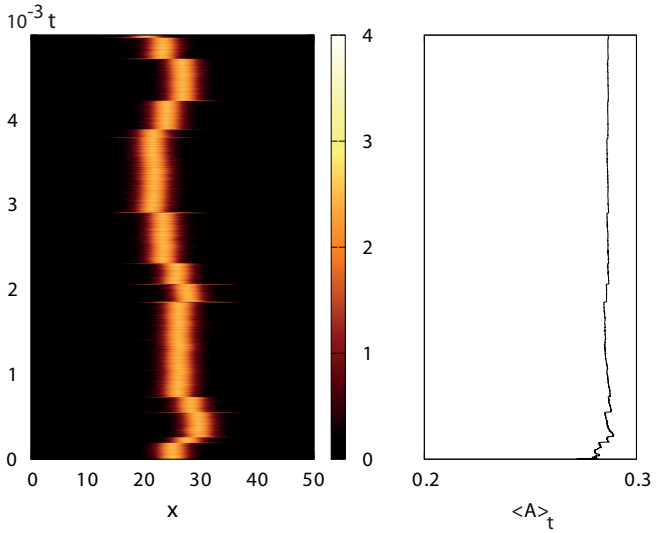

FIG. 1. $\eta_a = 0.01$, $\eta_m = 0.20$, $\langle A\rangle_T = 0.287$, $T = 5000$. The ordinate of the figure on the right has the same scale as the ordinate of the figure on the left.

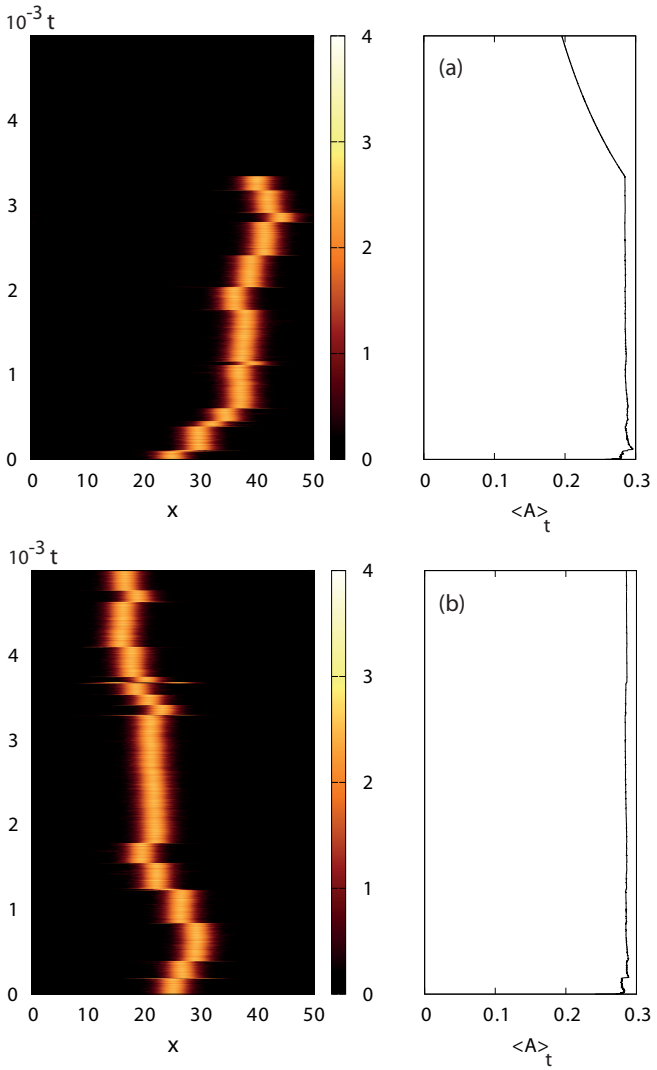

FIG. 2. $\eta_a = 0.01$, $\eta_m = 0.25$, $T = 5000$, (a) $\langle A\rangle_T = 0.1953$, (b) $\langle A\rangle_T = 0.2856$,

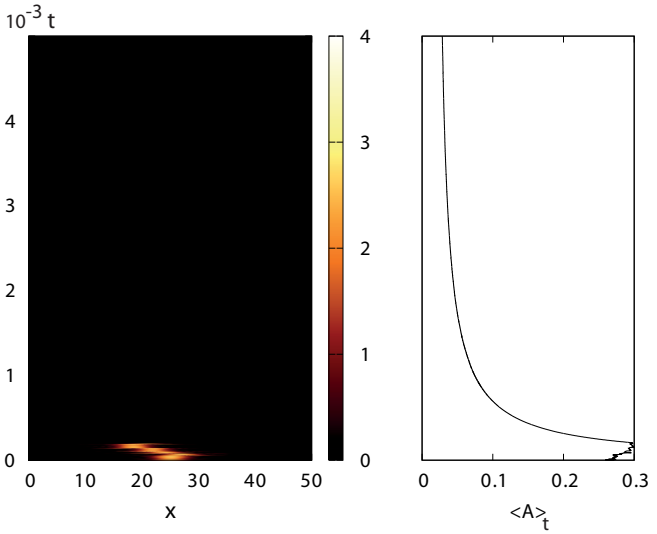

FIG. 3. $\eta_a = 0.01$, $\eta_m = 0.40$, $\langle A\rangle_T = 0.286$, $T = 5000$.

gas flux impinging on a sample for surface reactions typically leads to a combination of multiplicative and additive noise as has been discussed and analyzed theoretically and experimentally in Refs. [17–19]. The assumption of using additive noise, which is δ-correlated in space and time, deserves a word of caution. While this is surely well justifiable for thermal fluctuations, it can only be considered to be an approximation for noise that is nonthermal in origin, for example, related to vibrations in the setup. Near the onset of an instability the noise intensity found experimentally—compare, for example, the case of fluctuations below the onset of Rayleigh-Benard convection [25,26]—is several orders of magnitude larger than expected from thermal noise. In fact, the first experimental observation showing a noise intensity comparable to what is expected from thermal noise was reported by Rehberg *et al.* [27] for the case of electroconvection in thin cells of nematic liquid crystals near onset. Later it was also demonstrated near convective onset in a simple fluid [57] that the noise level of additive noise could be brought down to the level expected for thermal noise.

In our numerical simulations we keep all deterministic parameters fixed, while we vary the strengths of additive noise, η_a, and of multiplicative noise, η_m. The deterministic parameter values selected are for μ, the distance from linear onset, $\mu = -0.266$, for a large fraction of our studies, $\beta_r = 1$, $\beta_i = 0.8$, $\gamma_r = -0.1$, $\gamma_i = -0.6$, $D_r = 0.125$, and $D_i = 0.5$ (positive) corresponding to an anomalous dispersion regime for which exploding DSs can arise. Stable pulses can exist only when the CQGLE becomes nonvariational. Thus, at least one of the parameters (β_i, γ_i, D_i) must be different from zero [34,45,58,59]. We note that the value of μ has been chosen such that stationary pulses are stable. Nevertheless this value has been picked in a way that the transition of oscillatory DS with one frequency is quite close so that the system becomes more sensitive to noisy perturbations. To study the influence of the distance from the saddle node for stationary pulses on the one hand and from the onset of oscillatory DSs on the other we also investigated $\mu = -0.726$.

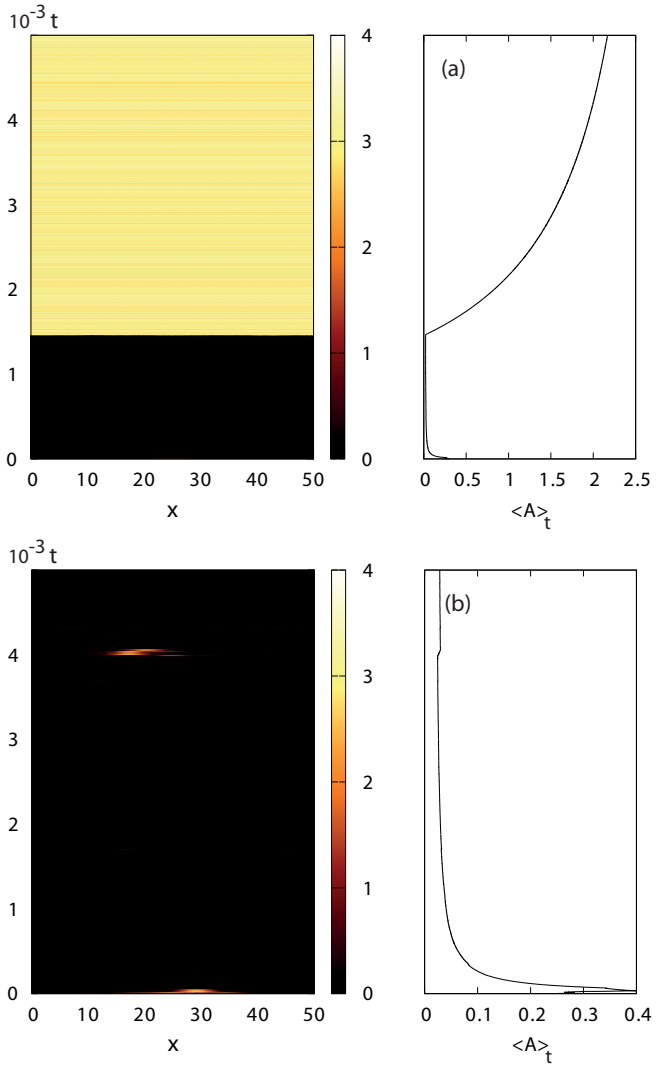

FIG. 4. $\eta_a = 0.01$, $\eta_m = 0.50$, $T = 5000$, (a) $\langle A \rangle_T = 2.168$, (b) $\langle A \rangle_T = 0.0285$. Note the difference in scale on the abscissa between panels (a) and (b).

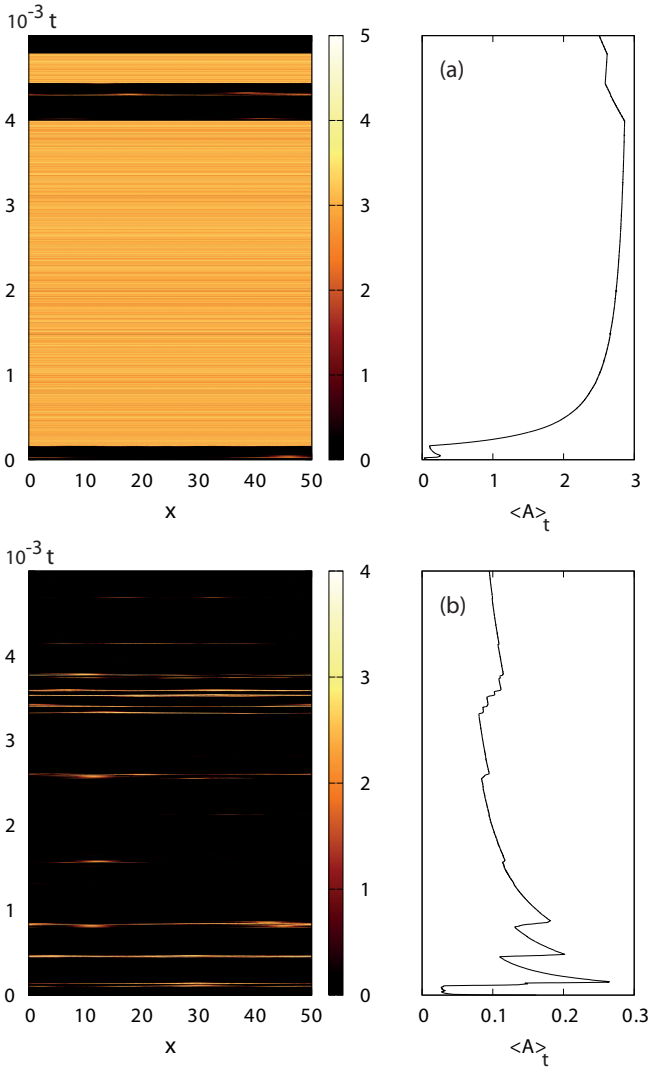

FIG. 5. $\eta_a = 0.01$, $\eta_m = 0.70$, $T = 5000$, (a) $\langle A \rangle_T = 2.504$, (b) $\langle A \rangle_T = 0.0950$. Note the difference in scale on the abscissa between panels (a) and (b).

In the discretized problem the stochastic force $\xi(t)$ associated with multiplicative noise is replaced by $\chi_r/\sqrt{dt}$, where χ_r corresponds to uncorrelated random numbers obeying a standard normal distribution; the stochastic force associated with additive noise, $\zeta(x,t)$, is replaced by $(\lambda_r + i\lambda_i)/\sqrt{dtdx}$, where λ_r and λ_i correspond to uncorrelated random numbers obeying standard normal distributions.

Throughout this work we will use the physically motivated Stratonovich interpretation of stochastic processes [3–5]. Surely, from a mathematical point of view, the Itô interpretation is also well established and described in detail in the literature for ordinary [60] as well as for partial stochastic differential equations [21,61]. It requires, however, that the rules of differential and integral calculus need to be redefined. Here we follow the "physical procedure" outlined, for example, in Ref. [4] and therefore use the Stratonovich interpretation, which allows one to retain the usual rules of differential calculus (compare, for example, Ref. [7] for zero-dimensional multiplicative stochastic processes as applied to statistical physics and nonlinear optics).

To perform the numerical simulations for Eq. (1) we implemented a split-step pseudospectral method where the differential operator is computed in Fourier space and the nonlinear terms are computed in the time step by using a fourth-order Runge-Kutta algorithm. The simulations were performed using $N = 625$ Fourier modes ensuring that even small scales are well solved.

This integration algorithm is similar to the stochastic second-order Heun method, commonly discussed in the literature [21,61]; the only differences are the values for the weight coefficients and the number of increments (four instead of two), which are computed in exactly the same way. Nevertheless, we used the fourth-order method because it gave us similar results to Heun's when integrating Eq. (1). We also previously used this same higher order scheme for the case with large additive noise [55] and a combination of additive and multiplicative noise [56], always obtaining

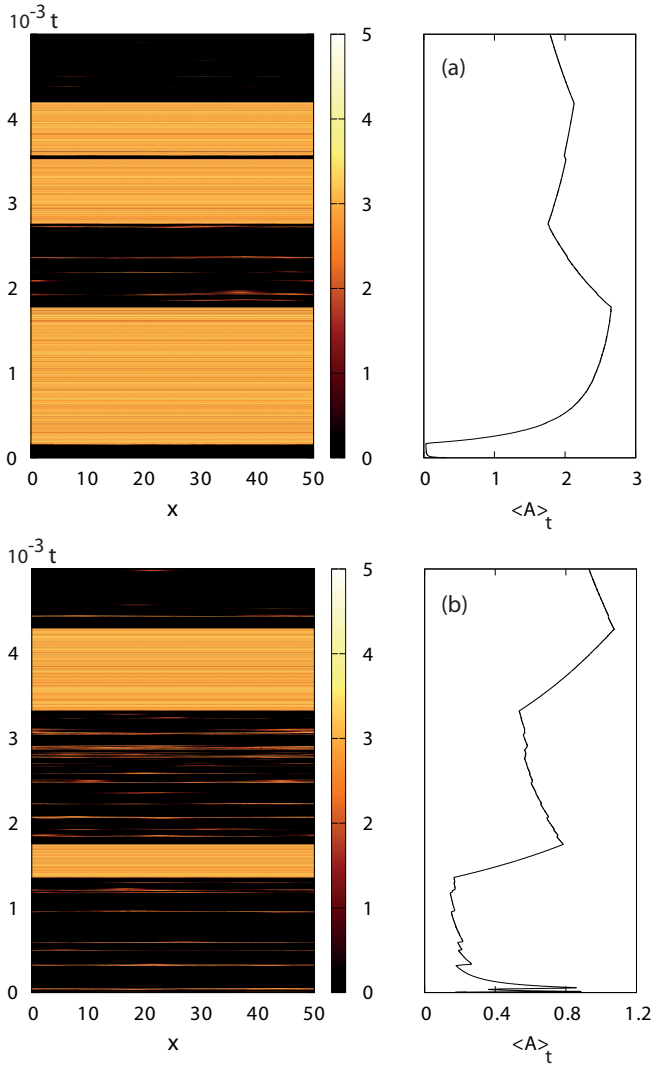

FIG. 6. $\eta_a = 0.01$, $\eta_m = 0.80$, $T = 5000$, (a) $\langle A\rangle_T = 1.7878$, (b) $\langle A\rangle_T = 0.9309$. Note the difference in scale on the abscissa between panels (a) and (b).

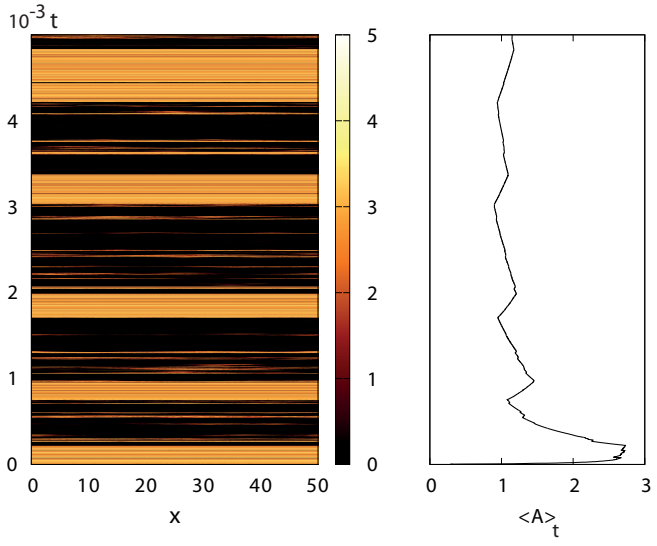

FIG. 7. $\eta_a = 0.01$, $\eta_m = 0.95$, $\langle A\rangle_T = 1.4740$, $T = 5000$.

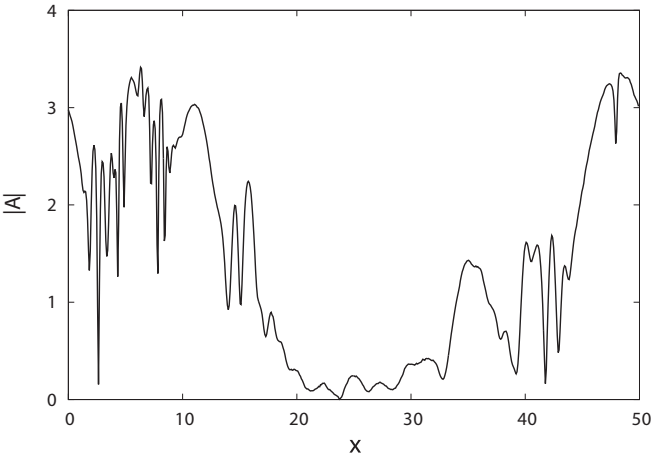

FIG. 8. Snapshot of spatio-temporal disordered behavior associated with Fig. 5(b): $\eta_a = 0.01$, $\eta_m = 0.70$, $t = 833$.

satisfactory results. Therefore we are confident that even if the fourth-order method is not the most time-efficient algorithm, it adequately solves Eq. (1).

To further ensure that our simulations were performed, using the right numerical parameters, we tried different values for the number of Fourier modes, from 256 to 2048, and the results were always consistent. Control runs for $dt = 0.005$ and $dt = 0.002$ as well as for varying N have also been performed to make sure that none of our results is sensitively dependent on this choice.

In parallel we carried out extensive numerical computations with an independent simulator of partial differential equations which uses as numerical method explicit fourth-order Runge-Kutta finite differencing with a grid of 625 points in x along a grid spacing of $dx = 0.08$ (corresponding to

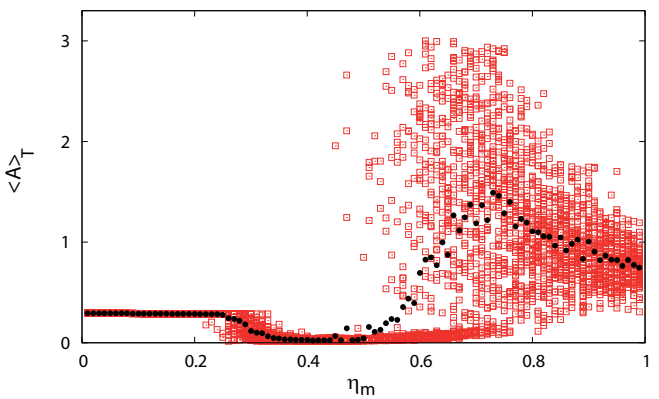

FIG. 9. Phase diagram for $\eta_a = 0.01$. η_m is varied from 0 to 1.00. Every open square corresponds to one run with $T = 5000$, and the phase diagram is obtained for 50 runs for every value of η_m. The black solid circles represent the Mean $\langle A\rangle$, the average over all runs performed for a fixed value of η_m. We note a fairly broad small-amplitude region for $\langle A\rangle_T$ versus η_m in the region around $\eta_m \sim 0.40$. As one can see for $0 < \eta_m < 0.55$ and for $0.85 < \eta_m < 1.00$ the black solid circles lie on a smooth curve, while for the interval $0.55 < \eta_m < 0.85$ also the average over 50 runs leads to a somewhat larger scatter in the averaged data.

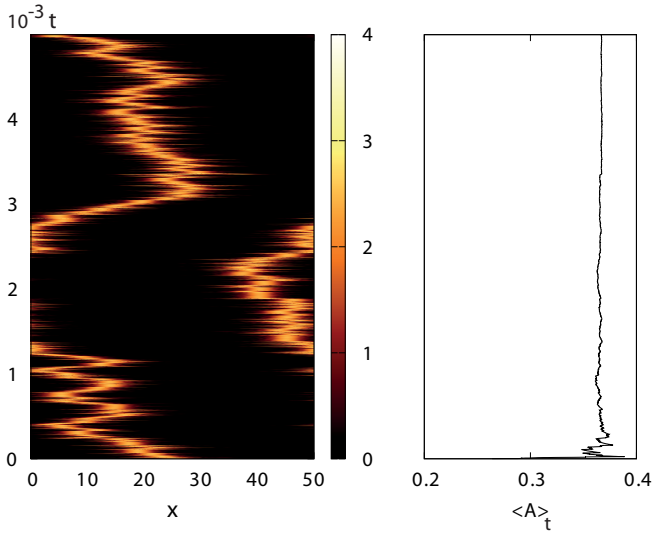

FIG. 10. $\eta_a = 0.03$, $\eta_m = 0.20$, $\langle A\rangle_T = 0.3667$, $T = 5000$.

a box size $L = 50$) and typical time steps dt were $dt = 0.005, 0.003$, and 0.002. The corresponding values for μ are $\mu = -0.24$ and -0.70. We used a maximum integration time $T = 2 \times 10^3$.

The initial conditions used on our simulations were generated by solving Eq. (1) with its corresponding value for $\mu(-0.266$ or $-0.726)$, without the stochastic forcing, for a total integration time $T = 2 \times 10^3$, to ensure the desired stationary behavior.

Finally, to characterize the noisy patterns quantitatively, we introduce $\langle A\rangle_t$, the average of $|A|$ in time and space:

$$\langle A\rangle_t = \frac{1}{Lt}\int_0^t \int_0^L |A|\, dx\, dt'. \tag{2}$$

To investigate the sensitivity of $\langle A\rangle_t$ the timescale of the runs was varied by more than one order of magnitude between $T = 2 \times 10^3$ and $T = 5 \times 10^4$. We verified that these changes do not lead to any significant changes. $\langle A\rangle_T$, averaged over a large number of realizations, which we will call Mean $\langle A\rangle$ throughout this paper, can thus be used as an order parameter, which varies smoothly as a function of the noise strength.

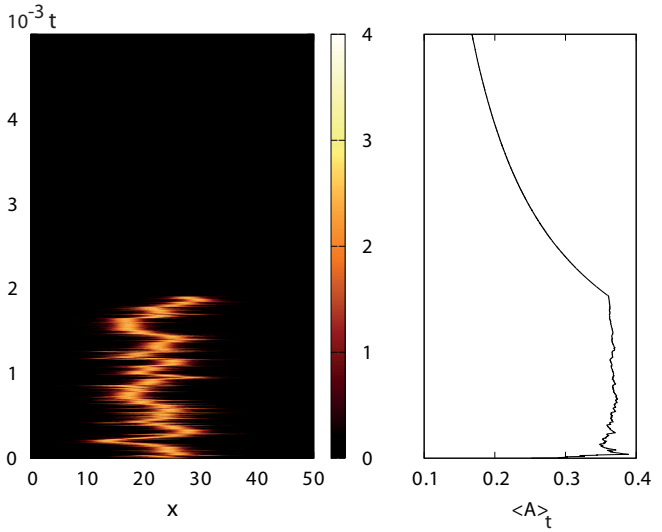

FIG. 11. $\eta_a = 0.03$, $\eta_m = 0.30$, $\langle A\rangle_T = 0.1676$, $T = 5000$.

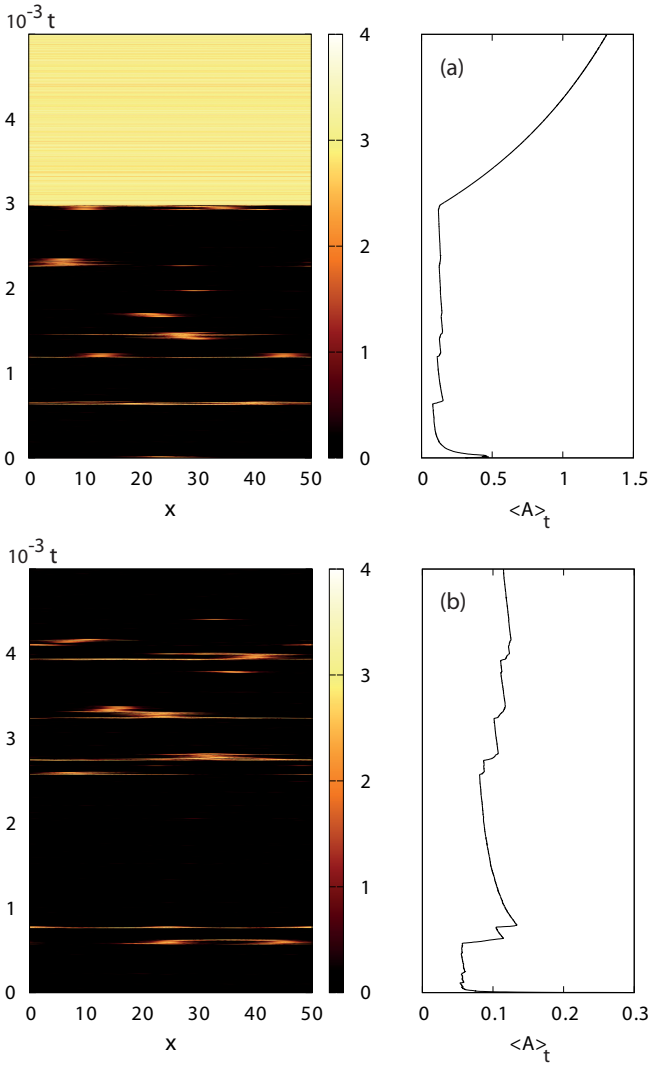

FIG. 12. $\eta_a = 0.03$, $\eta_m = 0.50$, $T = 5000$, (a) $\langle A\rangle_T = 1.3120$, (b) $\langle A\rangle_T = 0.1147$. Note the difference in scale on the abscissa between panels (a) and (b).

III. RESULTS AND DISCUSSION

A. Results and discussion for $\mu = -0.266$ and $\eta_a = 0.01$

We start with the presentation of x-t plots for the observed types of behavior for $\eta_a = 0.01$ and a fixed timescale $T = 5000$ after applying both types of noise to the initial conditions $A(x)$. In all x-t plots we show the spatial coordinate, x horizontally and the time, t, vertically, on the left and the average amplitude, $\langle A\rangle_t$ as a function of t on the right. In all x-t plots the ordinate of the figure on the right has the same scale as the ordinate of the figure on the left.

In Fig. 1 we show that for $\eta_m = 0.20$ meandering exploding dissipative solitons arise. This is also brought by the time evolution of the averaged amplitude on the right, which is almost constant.

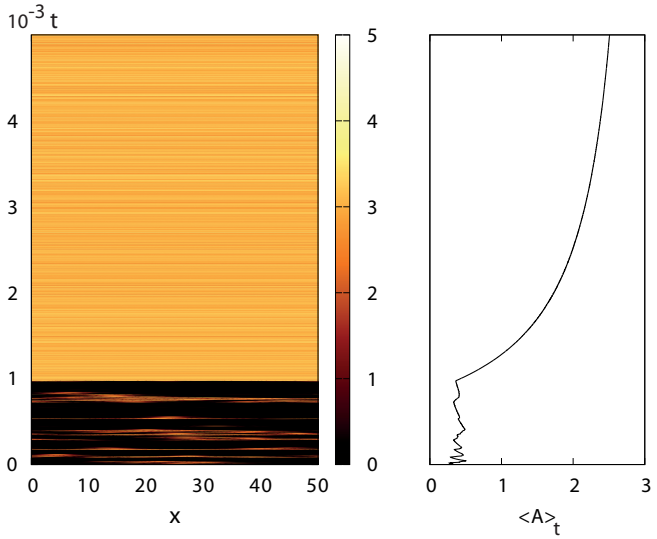

FIG. 13. $\eta_a = 0.03,\ \eta_m = 0.60,\ \langle A\rangle_T = 2.5081,\ T = 5000.$

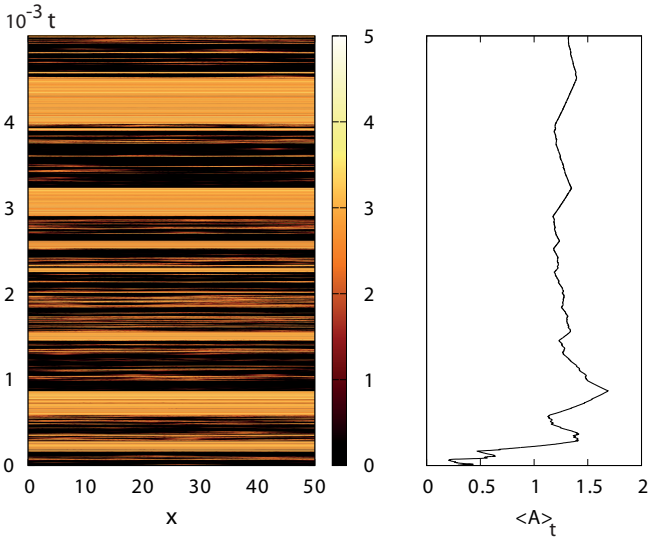

FIG. 15. $\eta_a = 0.03,\ \eta_m = 0.90,\ \langle A\rangle_T = 1.3249,\ T = 5000.$

This picture changes when increasing the amplitude of the multiplicative noise to $\eta_m = 0.25$. Now the final result of the run after $T = 5000$ can either be the noisy zero attractor shown in Fig. 2(a) or a meandering dissipative soliton shown in Fig. 2(b).

This type of behavior is followed by an interval of noise strengths for the multiplicative noise for which the noisy zero attractor prevails as shown in Fig. 3.

As η_m is increased further, we find a transition either to the noisy zero attractor or to filling in. This is shown in Fig. 4 for $\eta_m = 0.50$. We emphasize the different scale used in Fig. 4(a) and Fig. 4(b) for the abscissa showing $\langle A\rangle_t$.

As η_m goes up further intermittent behavior between two attractors (noisy zero and filled-in with noise or noisy zero and noise-induced disordered in time and space) is obtained as demonstrated in Fig. 5.

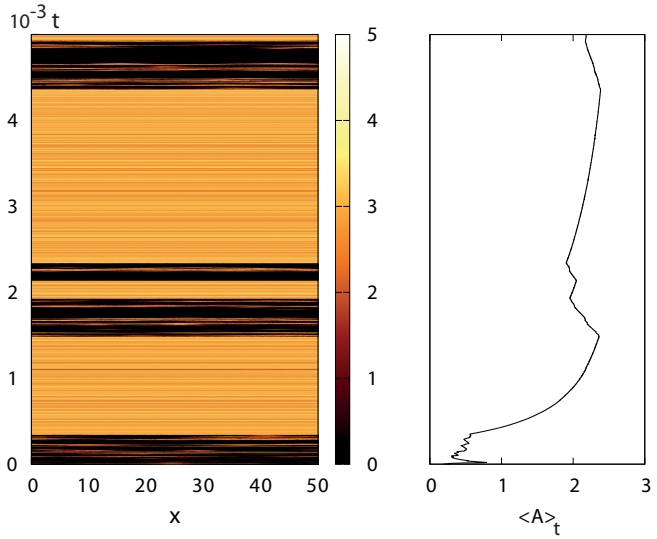

FIG. 14. $\eta_a = 0.03,\ \eta_m = 0.80,\ \langle A\rangle_T = 2.1843,\ T = 5000.$

For larger values of η_m $0.75 < \eta_m < 1.00$ one reaches a rather complex state with strongly intermittent behavior between noisy zero, disordered behavior in space and time, and filling in with noise.

This is brought out by the x-t plots and the time evolution of the averaged amplitude in Fig. 6 for $\eta_m = 0.70$ and in Fig. 7 for $\eta_m = 0.95$.

In Fig. 8 we show a snapshot of a short burst of disordered spatio-temporal behavior for $\eta_m = 0.70$ for a fixed time.

In Fig. 9 we show the phase diagram of $\langle A\rangle_T$ for $\eta_a = 0.01$ as a function of the strength of multiplicative noise η_m. A plateau-like region corresponding mainly to meandering exploding dissipative solitons is followed by an interval of multiplicative noise strengths for which collapse to the noisy zero attractor prevails. For larger noise strengths there is clearly

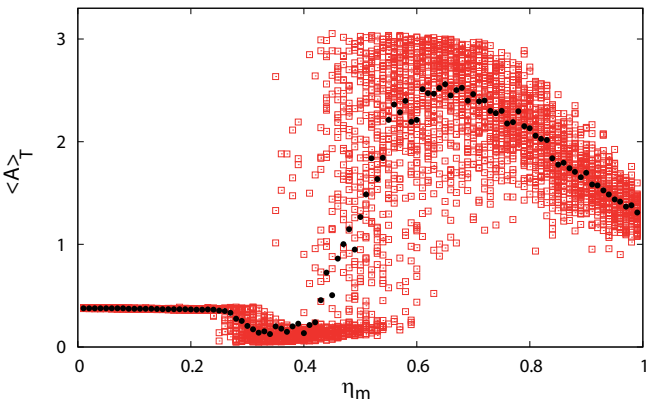

FIG. 16. Phase diagram for $\eta_a = 0.03$. η_m is varied from 0 to 1. Every open square corresponds to one run with $T = 5000$, and the phase diagram is obtained for 50 runs for every value of η_m. The black solid circles represent the average over all runs performed for a fixed value of η_m. As one can see for $0 < \eta_m < 0.55$ and for $0.80 < \eta_m < 1.00$ the black solid circles lie on a smooth curve, while for the interval $0.55 < \eta_m < 0.80$ also the average over 50 runs leads to a somewhat larger scatter in the averaged data.

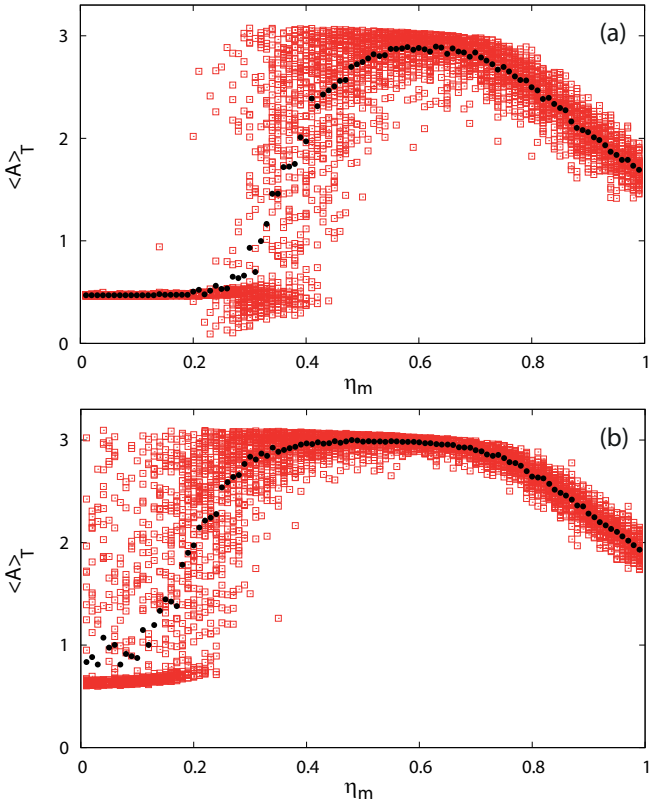

FIG. 17. Phase diagram for (a) $\eta_a = 0.05$ and (b) $\eta_a = 0.07$. η_m is varied from 0 to 1. Every open square corresponds to one run with $T = 5000$, and the phase diagram is obtained for 50 runs for every value of η_m. The black solid circles represent the average over all runs performed for a fixed value of η_m, that is, Mean $\langle A \rangle$. As one can see there is no longer a minimum in the $\langle A \rangle_T$ versus η_m curve, and the width of the small-amplitude plateau for small values of η_m is shrinking with increasing strength of additive noise. Instead a plateau for high amplitudes develops in the vicinity of $\eta_m \sim 0.60$ and broadens.

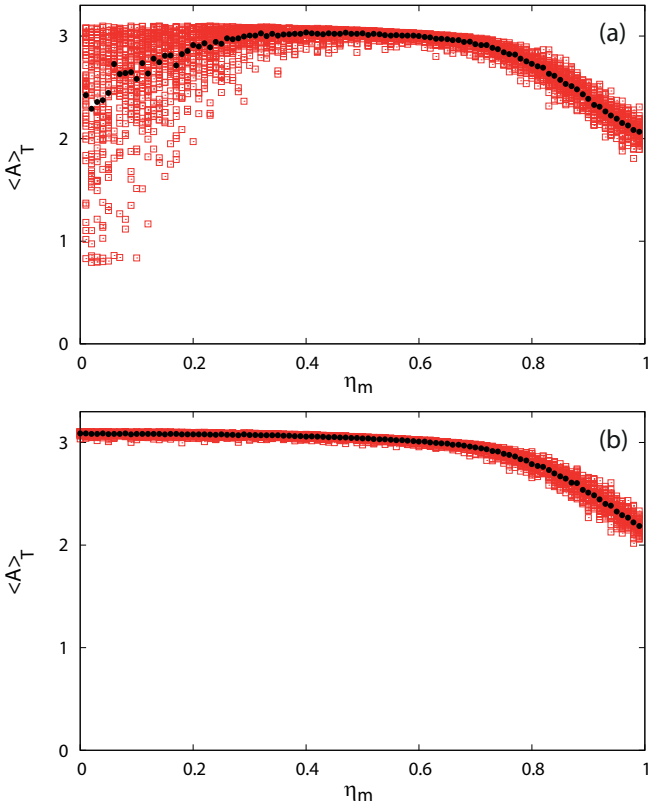

FIG. 18. Phase diagrams for (a) $\eta_a = 0.08$ and (b) $\eta_a = 0.10$. η_m is varied from 0 to 1. Every open square corresponds to one run with $T = 5000$, and the phase diagram is obtained for 50 runs for every value of η_m. The black solid circles represent the average over all runs performed for a fixed value of η_m, that is, Mean $\langle A \rangle$. As one can see the $\langle A \rangle_T$ versus η_m curve for $\eta_a = 0.10$ is now monotonically decaying after a long flat plateau starting essentially at $\eta_m = 0$.

a large dispersion in the data points reflecting the different types of behavior between different runs. Only for large noise strengths η_m does this dispersion decrease, indicating strongly intermittent behavior as a typical outcome.

To sum up we obtain the following types of behavior for $\mu = -0.266$ and $\eta_a = 0.01$:

(1) $0 < \eta_m < 0.25$: meandering of exploding solitons.

(2) $0.25 < \eta_m < 0.30$: system can evolve to meandering of exploding solitons or can go to the noisy zero attractor.

(3) $0.30 < \eta_m < 0.40$: system goes to the noisy zero attractor.

(4) $0.40 < \eta_m < 0.75$: system exhibits large time intervals in one of two noisy attractors: zero and filling in. Sometimes short bursts of disordered behavior in time and space are intercalated. Increasing $T_{\max}$ does not guarantee a settling to one attractor.

(5) $0.75 < \eta_m < 1.00$: strongly intermittent behavior. The system oscillates intermittently between the noisy zero attractor, disordered behavior, and filling in on a timescale of $\Delta T \sim 500, \ldots, 1000$.

B. Results and discussion for $\mu = -0.266$ and $\eta_a = 0.03$

To study the influence of a larger level of additive noise, we investigate $\eta_a = 0.03$. For $\eta_m = 0.20$ we find a rapid meandering of explosive dissipative solitons (Fig. 10), and for $\eta_m = 0.30$ rapidly meandering dissipative solitons die fairly quickly (Fig. 11).

For larger values of η_m, $0.30 < \eta_m < 0.50$, the system shows three types of behavior: it goes to the noisy zero attractor very quickly and stays there; alternatively it exhibits some degree of intermittency between disordered behavior and the noisy zero attractor [Fig. 12(b)]. Third, it can jump to the upper attractor. Once the upper attractor is reached [Fig. 12(a)], and it stays there for $T \sim 5 \times 10^4$.

As η_m is increased further ($0.5 < \eta_m < 0.7$) the system moves to the upper attractor and stays there (compare, for example, Fig. 13).

Upon further increase of the strength of multiplicative noise ($0.7 < \eta_m < 1.0$) the system oscillates intermittently between the noisy zero attractor, disordered behavior, and filling in with a typical timescale of $\Delta T = 300, \ldots, 10^3$ (compare Figs. 14 and 15).

In Fig. 16 we show the phase diagram of $\langle A \rangle_T$ for $\eta_a = 0.03$ as a function of the strength of multiplicative noise η_m. As for $\eta_a = 0.01$ a plateau-like region corresponding mainly

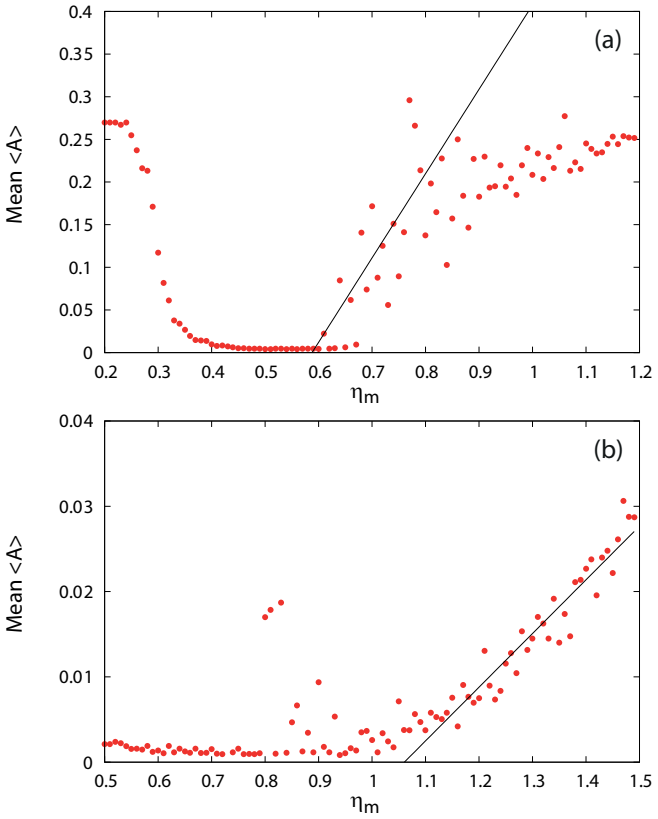

FIG. 19. Mean $\langle A\rangle$ versus η_m, for (a) $\eta_a = 0.001$ and (b) $\eta_a = 10^{-7}$ (for $\mu = -0.266$ and 50 runs for each value of η_m). The solid lines are used to determine the jump location by extrapolation.

to meandering exploding dissipative solitons is followed by an interval of multiplicative noise strengths for which collapse to the noisy zero attractor prevails. We note that the latter region has shrunk in size and that the larger value of η_a leads to a nonzero value for $\langle A\rangle_T$. As η_m increases there is clearly a broader region with large dispersion in the data points reflecting the easier access to different types of behavior

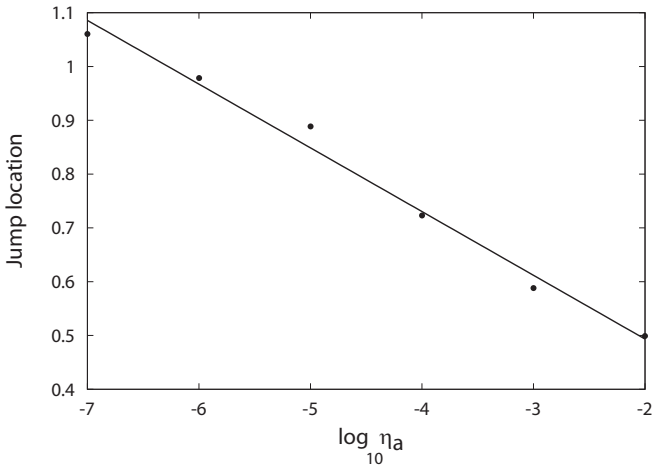

FIG. 20. The location of the start of the finite amplitude branch due to the presence of multiplicative noise is plotted as a function of the strength of additive noise, η_a

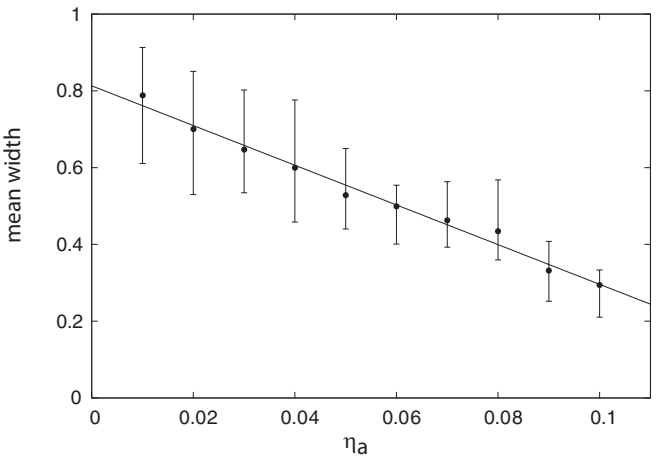

FIG. 21. The mean width of the amplitude is plotted as a function of η_a in the limit $\eta_m \to 1.0$.

between different runs for a larger level of additive noise. For large noise strengths η_m this dispersion reduces again, but not as much as for the case of weaker additive noise.

In summary we find the following types of behavior for $\mu = -0.266$ and $\eta_a = 0.03$:

(1) $0 < \eta_m < 0.25$: rapid meandering of exploding solitons.

(2) $0.25 < \eta_m < 0.30$: system goes to the noisy zero attractor before $T = 5000$.

(3) $0.30 < \eta_m < 0.50$: system goes to the noisy zero attractor very quickly and stays there; alternatively it exhibits some degree of intermittency between disordered behavior and the noisy zero attractor. Third, it can jump to the upper attractor. Once the upper attractor is reached, it stays there for $T \sim 5 \times 10^4$.

(4) $0.50 < \eta_m < 0.70$: for time intervals up to $T = 5000$ the system moves to the upper attractor and stays there.

(5) $0.70 < \eta_m < 1.00$: the system oscillates intermittently between the noisy zero attractor, disordered behavior and filling in with a typical timescale of $\Delta T = 300, \ldots, 10^3$.

C. Phase diagrams for $\langle A\rangle$ versus η_m as a function of η_a

In Figs. 9 and 16 we have presented the phase diagrams $\langle A\rangle_T$ versus η_m for fairly small values of the additive noise. Here we present complementary results for $\eta_a = 0.05$ to $\eta_a = 1.00$ in Figs. 17 and 18. With increasing strength of the additive noise the plateau at small multiplicative noise associated with meandering exploding DSs gradually disappears and eventually around $\eta_a \sim 0.09$ the transition to a filling-in state with noise dominates even for small values of multiplicative noise. The noisy zero solution observed for moderate strengths of the multiplicative noise (near $\eta_m \sim 0.40$) is already gone for $\eta_m = 0.05$. Instead a broad plateau associated with filling-in solutions starts to arise at $\eta_a = 0.05$ and eventually broadens and dominates even near η_m close to zero corresponding to the transition to filling in for exploding DSs for $\eta_m = 0$.

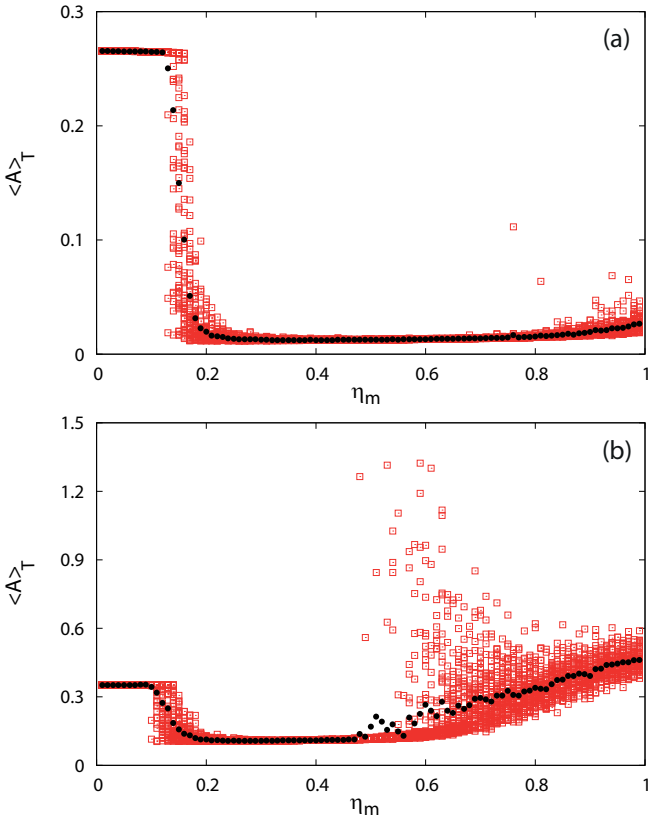

FIG. 22. The average value of the amplitude, Mean $\langle A\rangle$ as well as $\langle A\rangle_T$ for $\mu = -0.726$ are plotted for two values η_a: (a) $\eta_a = 0.01$ and (b) $\eta_a = 0.09$.

D. The limit of small additive noise

From the studies of the effects of multiplicative noise it is well known that the limit of small additional additive noise is quite subtle [7,8]. Therefore we have looked into this question for the case studied here, namely, the influence of simultaneous multiplicative and additive noise on stationary dissipative solitons.

To investigate these effects we varied η_a from $\eta_a = 0.01$ to $\eta_a = 10^{-7}$ and determined the resulting phase diagrams.

To analyze our data we have extracted the intercept for the various values of η_a for which the finite amplitude branch as a function of η_m is starting to grow. This procedure is indicated in Fig. 19. We emphasize that the finite value for the plateau in the amplitude for $\eta_m \to 0$ is related to the existence of exploding DSs and is therefore unrelated to the effects of multiplicative noise dominant at a larger value of η_m,

In Fig. 20 we have plotted the location of the jump in slope for multiplicative noise, η_m, as a function of the logarithm of the strength of additive noise, η_a. We clearly see that this plot has a linear negative slope: to trigger the onset of the finite amplitude branch induced by multiplicative noise scales with the logarithm of the amount of additive noise needed. We interpret this result in the spirit of the Kramers picture for the escape over a potential barrier, in our case for the simultaneous influence of additive as well as multiplicative noise on stationary DSs. A somewhat related result has been found for the lifetime of a localized solution of any length

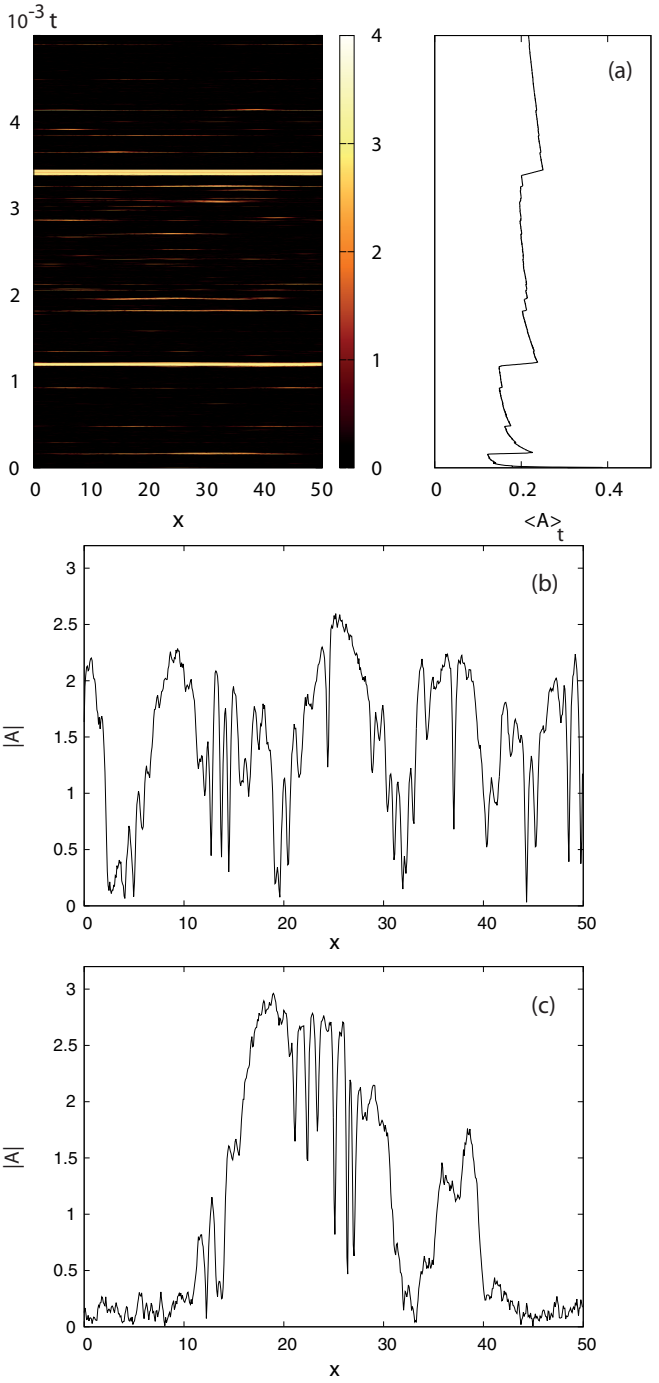

FIG. 23. x-t plot (a) and snapshots for $\mu = -0.726$, $\eta_a = 0.09$, $\eta_m = 0.70$, $\langle A\rangle_T = 0.2169$, $T = 5000$. The two snapshots of spatio-temporal disordered behavior are for (b) $T = 1812$ and (c) $T = 1958$.

for the cubic-quintic Swift-Hohenberg equation with additive noise [62].

Complementing the information given so far we have plotted the mean width of the amplitude, $\langle A\rangle_T$, as a function of the strength of the additive noise, η_a, in the limit $\eta_m \to 1$ in Fig. 21. The error bars are obtained by averaging over 50 runs of $T = 5000$ each. A linear decay of the mean width is clearly discernible.

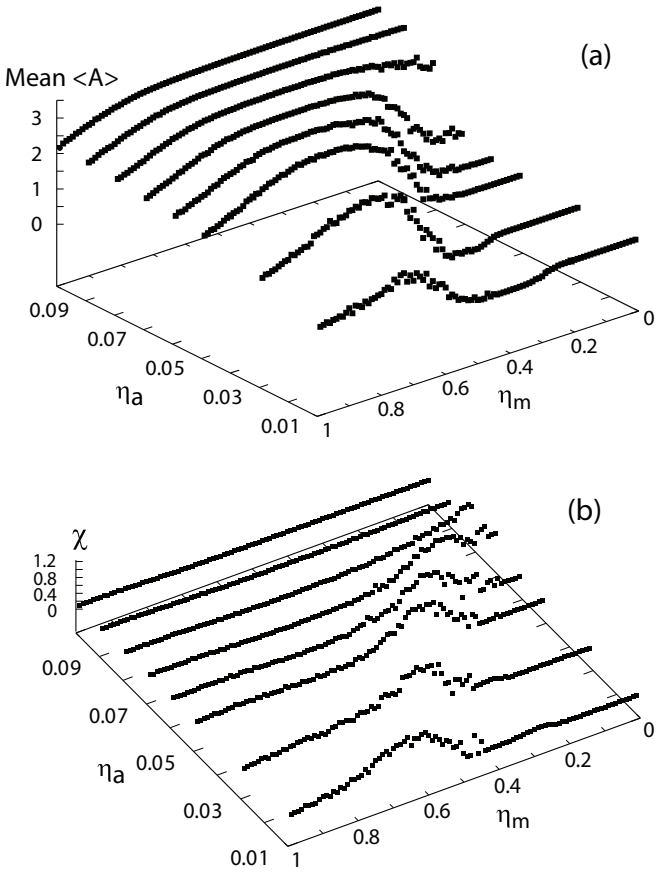

FIG. 24. The mean amplitude, Mean $\langle A\rangle$ (a) and the susceptibility χ are plotted for $\mu = -0.266$ as a function of the strength of multiplicative noise η_m and additive noise η_a. We note the different scales on the Mean $\langle A\rangle$ and χ axes.

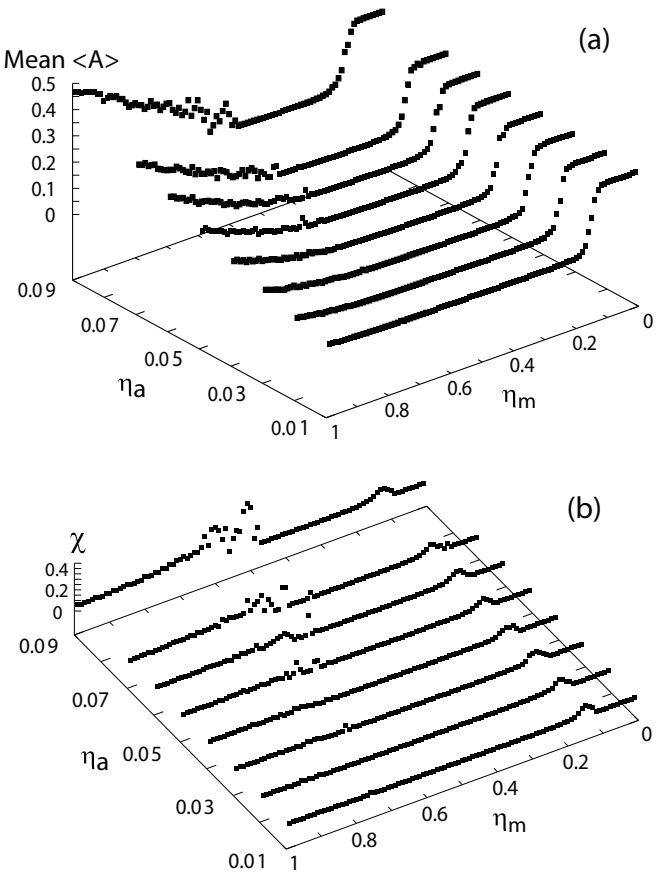

FIG. 25. The mean amplitude, Mean $\langle A\rangle$ (a) and the susceptibility χ are plotted for $\mu = -0.726$ as a function of the strength of multiplicative noise η_m and additive noise η_a. We note the different scales on the Mean $\langle A\rangle$ and χ axes.

E. Results and discussion for $\mu = -0.726$: Phase diagrams

To discuss the influence of the distance from the saddle node for DSs on the effects of multiplicative noise we have chosen a value of $\mu = -0.726$, which is about half way between the μ value we have discussed ($\mu = -0.266$) and the location of the saddle node for the existence of stationary DSs. While we have scanned the same range of values for η_a as for the previous μ, we present in Fig. 22 the phase diagrams for $\eta_a = 0.01$ and $\eta_a = 0.09$. From inspection of Fig. 22 it emerges that the slope of the curve $\langle A\rangle_T$ versus the strength of the multiplicative noise is much smaller than for $\mu = -0.266$ and that also the η_m value for which one starts to get a significant contribution to $\langle A\rangle_T$ is much higher for fixed η_a when going from $\mu = -0.226$ to $\mu = -0.726$. This goes well with the intuition that the basin of attraction for the finite amplitude branch is much deeper for $\mu = -0.726$ than for $\mu = -0.266$.

For $\mu = -0.726$ we expect qualitatively the same phase diagram for normal dispersion because the $\mu-$value is sufficiently far away in μ from the occurrence of exploding dissipative DSs.

In Fig. 23 we present a typical x-t plot for $\eta_a = 0.09$ and two snapshots taken from this run demonstrating spatio-temporal disorder, which appears intermittently.

IV. COMPARISON OF THE RESULTS TO THE CASES OF PURELY ADDITIVE AND PURELY MULTIPLICATIVE NOISE

In this section we critically compare how the results for the simultaneous presence of additive and multiplicative noise are different from the observations known for purely additive or purely multiplicative noise. Throughout this paper we have focused on two values for the distance from the linear onset of the instability, μ, namely, predominantly $\mu = -0.266$ and on $\mu = -0.726$, which is located about half way between the saddle node for deterministically stable stationary DSs and the their transition to oscillatory DSs.

To set the stage we briefly summarize the phenomena known for the separate effects of additive and multiplicative noise on deterministically stable stationary DSs. First, it is known [53] that a small amount of additive noise $10^{-7} < \eta_a < 10^{-2}$ can lead to the partial annihilation of colliding stationary DSs, a phenomenon that has been experimentally observed [43,63–65]. Second, we have shown [55] that large additive noise applied to a system below the saddle node for stationary DSs can be used to induce noisy localized solutions or filling in as long as there is a spatially homogeneous finite amplitude branch. Most relevant here for comparison purposes is the case we have studied in Ref. [54]. A relatively small amount

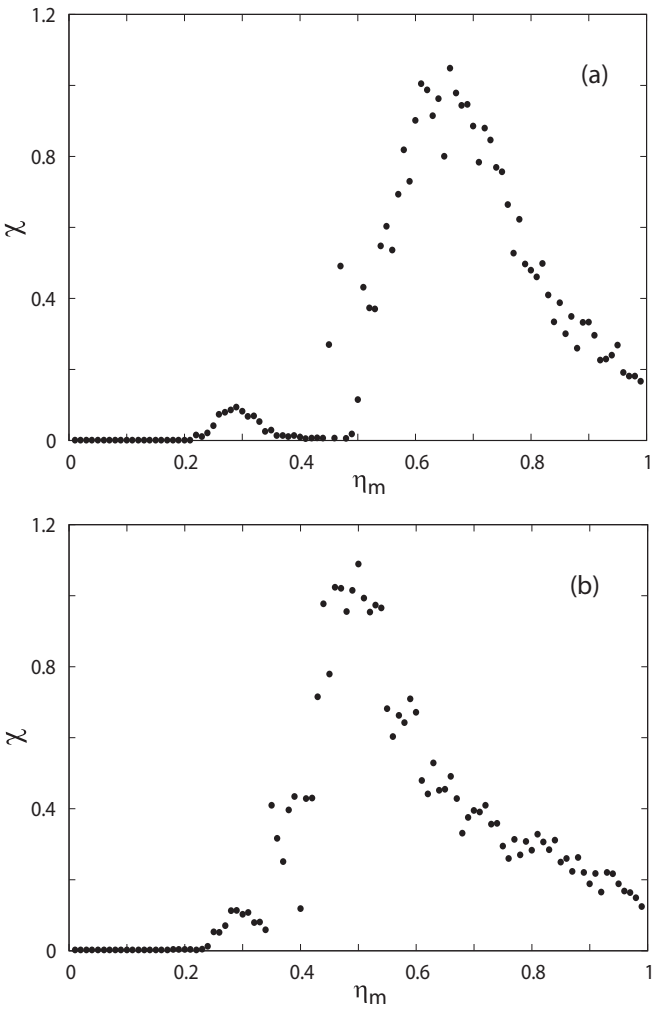

FIG. 26. The susceptibility χ is plotted for $\mu = -0.266$ as a function of the strength of multiplicative noise η_m for (a) $\eta_a = 0.01$ and (b) $\eta_a = 0.03$.

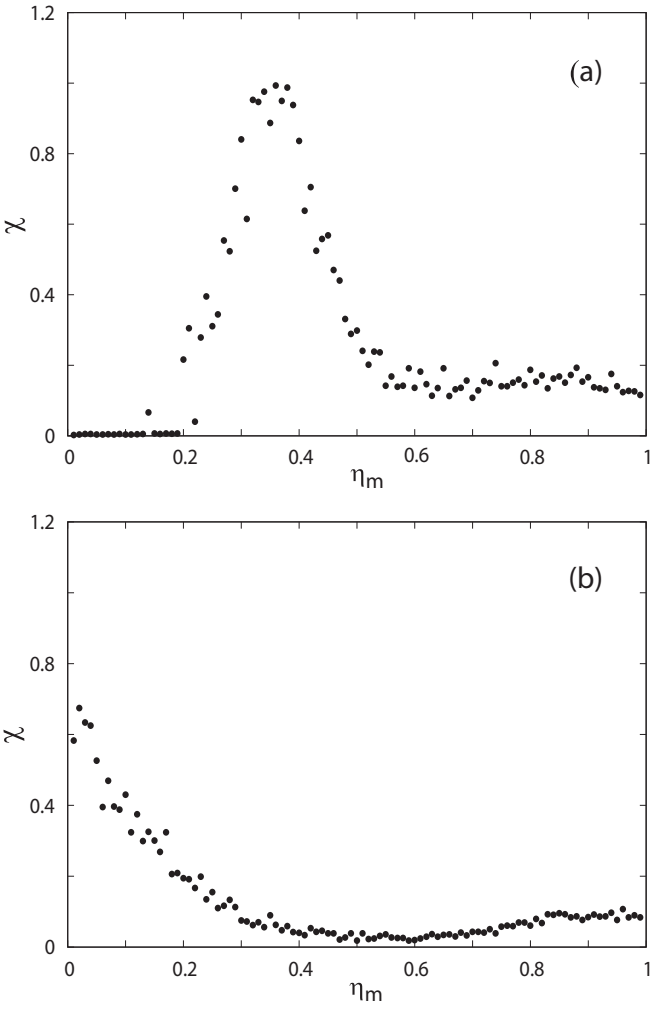

FIG. 27. The susceptibility χ is plotted for $\mu = -0.266$ as a function of the strength of multiplicative noise η_m for (a) $\eta_a = 0.05$ and (b) $\eta_a = 0.08$.

of additive noise ∼1% is able to induce chaotic explosions for the regime of subcriticality, which is close to the onset of temporally varying deterministic DSs but still shows stationary DSs. As for spatially homogeneous purely multiplicative noise we have shown [56] that one can stabilize the noisy zero solution for moderately large values of the strength of multiplicative noise down to the saddle node for stationary deterministic DSs. Also oscillatory DSs can be postponed in their onset. For exploding DSs one can observe for spatially homogeneous multiplicative noise collapse, filling in, and persistent explosions as a function of the strength of η_m. We note that we did not observe intermittent switching between filling in and noisy zero for spatially homogeneous purely multiplicative noise.

In this article we find as an additional scenario, for small values of additive noise $\eta_a \sim 0.01 \ldots 0.03$ and the simultaneous presence of moderate values of spatially homogeneous multiplicative noise, strongly intermittent behavior between the noisy zero attractor, filling in, and spatio-temporal disorder. For fixed additive noise varying the strength of multiplicative noise one can induce transitions from explosions to noisy zero and then to filling in as η_m increases. When increasing η_a from 0.01 to 0.03 a rapid meandering of exploding DSs is obtained.

The limit of small additive noise (or equivalently of a small ratio η_a/η_m) is also quite subtle for the application of noise to DSs. In this context it has been shown early on for the case of spatially homogeneous systems that even a small amount of additive noise leads to an exponential decay of correlation functions, while for purely multiplicative noise an algebraic decay of correlation functions emerges [8], thus indicating a rather singular limit. For the case of stationary DSs we also find a quite delicate behavior in the limit of small η_a/η_m. The location for the onset of the finite amplitude branch due to multiplicative noise depends logarithmically on the strength of additive noise over more than five decades of η_a (from about $\eta_a \sim 10^{-2}$ to $\eta_a \sim 10^{-7}$). In addition, as η_a grows, the regime with noisy zero disappears and is replaced by filling in: above $\eta_a \sim 0.07$ meandering explosions disappear altogether. It also appears worth notice that the width of the finite amplitude branch decreases on the average linearly with increasing values of η_a.

Increasing the distance from linear onset to $\mu = -0.726$ we have demonstrated that a much larger value for the amplitude of the multiplicative noise, η_m (for fixed strength of the additive noise, η_a) is needed to reach the finite amplitude (filling-in) branch. This behavior is closely associated with the fact that the basin of attraction for deterministic stationary DSs is becoming much deeper and narrower as the value of μ is reduced.

V. GENERAL PICTURE: NOISE-INDUCED PHASE TRANSITIONS

The aim of this section is to show a general picture of the simultaneous influence of additive and multiplicative noise on stationary dissipative solitons, which summarizes the main features shown in the previous sections.

In nonequilibrium phase transitions the usual partition-function methodology cannot be applied. However, measures like order parameters and generalized susceptibilities can still be calculated from statistical (spatial and temporal) averages of the order parameter.

To characterize equilibrium phase transitions as well as transitions far from equilibrium using the averaged order parameter and the corresponding susceptibilities is a well-documented approach in the literature. For details we refer, for example, to Refs. [66,67] for the equilibrium case and to Refs. [21,68] for nonequilibrium situations.

The order parameter we use is Mean $\langle A \rangle$, $\langle A \rangle_T$ averaged over a large number of realizations. For the generalized susceptibility χ we have [6,21]

$$\chi \sim \langle (\langle A \rangle_T)^2 \rangle - \langle \langle A \rangle_T \rangle^2. \tag{3}$$

In Figs. 24 and 25 we give an overview of our results for Mean $\langle A \rangle$ and χ for $\mu = -0.266$ and $\mu = -0.726$. Figure 24(a) is a three-dimensional plot showing Mean $\langle A \rangle$ for $\mu = -0.266$ as a function of the strength of multiplicative noise η_m and additive noise η_a. We observe that for small η_a and small η_m the Mean $\langle A \rangle$ exhibits a plateau corresponding to meandering exploding dissipative solitons (in Ref. [54] we have shown that small additive noise can induce explosions), whose extension decreases monotonically giving rise to a noise-induced phase transition to a noisy filling-in solution as η_a increases.

For small strengths of additive noise η_a one notices another noise-induced phase transition: from the above-mentioned plateau to the noisy zero solution by increasing the multiplicative noise η_m. Its collapse is reminiscent of the result found in Ref. [56]; that is, large multiplicative noise can lead to the suppression of dissipative solitons for zero additive noise. This transition is clearly captured by the generalized susceptibility χ, as is shown by the small peaks in Fig. 26.

A third noise-induced phase transition shown in this three-dimensional plot is that from the noisy zero solution to filling in, as η_m increases, for fixed additive noise. The large peaks in Figs. 26 and 27 characterize these transitions. All the above described noise-induced phase transitions are continuous. Figure 24 offers a general picture (Mean $\langle A \rangle$ and the generalized susceptibility χ) of the phases and noise-induced phase transitions in the (η_m, η_a) space for $\mu = -0.266$.

For $\mu = -0.726$, which is about half way between $\mu = -0.266$ and the location of the saddle node for the existence of stationary DSs, Fig. 25 provides a general overview by plotting the mean value of the amplitude and the generalized susceptibility χ as a function of the strength of multiplicative noise η_m and additive noise η_a. From Fig. 25(a) we see that for the whole range of additive noise η_a the system starts with a plateau corresponding to noisy stationary solitons. When increasing the strength of the multiplicative noise η_m the system experiences a noise-induced phase transition to a noisy zero solution. As η_m is increased further, we find a transition to filling in. Transitions are captured by the generalized susceptibility χ shown in Fig. 25(b). Qualitative differences between Fig. 24 and Fig. 25 rely on the fact that the basin of attraction for deterministic stationary dissipative solitons becomes deeper when μ goes from -0.266 to -0.726.

VI. CONCLUSIONS AND PERSPECTIVE

In conclusion, we have investigated the simultaneous influence of spatially homogeneous multiplicative noise as well as of spatially δ-correlated additive noise on the formation of localized patterns in the framework of the cubic-quintic complex Ginzburg-Landau equation. This study of driven dissipative systems was motivated by the fact that one can apply multiplicative noise in a controlled way to a broad range of experimental systems including electroconvection in nematic liquid crystals, thermal convection in fluids, and chemical reactions on surfaces under ultrahigh vacuum conditions. Additive noise of various sources and a strength which can vary several orders of magnitude is always inevitable in a real experimental system.

Depending on the ratio between the strength of additive and multiplicative noise we find a number of distinctly different types of behavior including explosions, collapse, filling in, and spatio-temporally disordered behavior. In particular we find, for fixed strengths of the additive and the multiplicative noise, a type of intermittent behavior not described before: filling in, the noisy zero solution, and a spatio-temporally disordered patterns emerge and disappear as a function of time indefinitely.

Techniques used to analyze the results include snapshots, x-t plots, and plots of the spatially and temporally averaged amplitude as a function of the strength of multiplicative noise while keeping the strength of additive noise fixed. Typically 50 realizations were used for averaging to obtain the corresponding data points in these diagrams. For the widths of these distribution as a function of additive noise we obtain a linear decrease in the limit of fairly large, but fixed values of the multiplicative noise. We have critically compared the results obtained with those obtained in the two limiting cases of purely additive and of purely multiplicative noise. We have demonstrated that spatially homogeneous multiplicative noise can induce a transition to a noisy spatially homogeneous state for a range of the bifurcation parameter for stationary DSs in the presence of additive noise, while this is not possible without additive noise.

In order to present a concise overall summary of our investigations we have included three-dimensional plots of the order parameter (the mean pattern amplitude) and the generalized susceptibility χ as a function of the strength of additive and multiplicative noise, respectively. To elucidate

further the importance of the generalized susceptibility for the characterization of the transitions between different patterns we have also incorporated plots showing χ as a function of the strength of multiplicative noise for various fixed values of the strength of additive noise.

Clearly there are several directions into which the presented results can be generalized. As we have focused here on spatial variations in one dimension, an obvious possibility is to consider two-dimensional systems, which are also experimentally relevant ranging from fluid dynamics over chemical reactions to biological dynamics. In the present paper we have concentrated on the effects of noise on stationary dissipative solitons. Clearly time-dependent DSs as well as explosive DSs are expected to be rather sensitive to noisy perturbations and as such will be a natural field to investigate. This applies in particular to the dynamics of explosive DSs whose deterministic dynamics has been characterized theoretically in one and two spatial dimensions [69–73]. We note in passing that in this connection the question of anomalous diffusion of DSs in the complex CQGLE, in two spatial dimensions has been studied [73,74] as well. Keeping in mind that in some fields (including chemical reactions and nonlinear optics) other types of nonlinearities including saturation nonlinearities and nonlinear gradient terms play a role, this area emerges naturally as an additional direction to go into regarding the study of the simultaneous presence of additive and spatially homogeneous multiplicative noise, as it is typically applied experimentally externally.

ACKNOWLEDGMENTS

O.D. and C.C. wish to acknowledge the support of FONDECYT (CL), 1170728 and Universidad de los Andes (CL) through FAI initiatives. H.R.B. thanks the Deutsche Forschungsgemeinschaft (DE) for partial support of this work.

[1] L. S. Tsimring, Rep. Prog. Phys. **77**, 026601 (2014).
[2] I. Hecht, D. A. Kessler, and H. Levine, Phys. Rev. Lett. **104**, 158301 (2010).
[3] N. G. van Kampen, *Stochastic Processes in Physics and Chemistry* (North-Holland, Amsterdam, 1983).
[4] H. Risken, *The Fokker-Planck Equation* (Springer, Berlin, 1989).
[5] C. W. Gardiner, *Handbook of Stochastic Methods* (Springer, Berlin, 1989).
[6] R. Graham, Phys. Rev. A **10**, 1762 (1974).
[7] A. Schenzle and H. Brand, Phys. Rev. A **20**, 1628 (1979).
[8] H. R. Brand, Prog. Theor. Phys. **72**, 1255 (1984).
[9] S. Wehner, S. Karpitschka, Y. Burkov, D. Schmeisser, J. Küppers, and H. R. Brand, Physica D **239**, 746 (2010).
[10] S. Kabashima, S. Kogure, T. Kawakubo, and T. Okada, J. Appl. Phys. **50**, 6296 (1979).
[11] K. Kaminishi, R. Roy, R. Short, and L. Mandel, Phys. Rev. A **24**, 370 (1981).
[12] R. Graham, M. Höhnerbach, and A. Schenzle, Phys. Rev. Lett. **48**, 1396 (1982).
[13] R. Lefever and J. W. Turner, Phys. Rev. Lett. **56**, 1631 (1986).
[14] L. Fronzoni, R. Mannella, P. V. E. McClintock, and F. Moss, Phys. Rev. A **36**, 834 (1987).
[15] I. Bashkirtseva, T. Ryazanova, and L. Ryashko, Phys. Rev. E **92**, 042908 (2015).
[16] S. Wehner, Y. Hayase, H. R. Brand, and J. Kuppers, J. Phys. Chem. B **108**, 14452 (2004).
[17] Y. Hayase, S. Wehner, J. Kuppers, and H. R. Brand, Phys. Rev. E **69**, 021609 (2004).
[18] S. Wehner, P. Hoffmann, D. Schmeisser, H. R. Brand, and J. Kuppers, Phys. Rev. Lett. **95**, 038301 (2005).
[19] P. Hoffmann, S. Wehner, D. Schmeisser, H. R. Brand, and J. Kuppers, Phys. Rev. E **73**, 056123 (2006).
[20] S. Wehner, P. Hoffmann, D. Schmeisser, H. R. Brand, and J. Kuppers, Chem. Phys. Lett. **423**, 39 (2006).
[21] F. Sagués, J. M. Sancho, and J. García-Ojalvo, Rev. Mod. Phys. **79**, 829 (2007).
[22] S. Alonso, I. Sendiña-Nadal, V. Pérez-Muñuzuri, J. M. Sancho, and F. Sagués, Phys. Rev. Lett. **87**, 078302 (2001).
[23] P. S. Bodega, S. Alonso, and H. H. Rotermund, J. Chem. Phys. **130**, 084704 (2009).
[24] P. Manneville, *Dissipative Structures and Weak Turbulence* (Academic Press, London, 1990).
[25] C. W. Meyer, G. Ahlers, and D. S. Cannell, Phys. Rev. Lett. **59**, 1577 (1987).
[26] C. W. Meyer, G. Ahlers, and D. S. Cannell, Phys. Rev. A **44**, 2514 (1991).
[27] I. Rehberg, S. Rasenat, M. de la Torre Juárez, W. Schöpf, F. Hörner, G. Ahlers, and H. R. Brand, Phys. Rev. Lett. **67**, 596 (1991).
[28] H. R. Brand, S. Kai, and S. Wakabayashi, Phys. Rev. Lett. **54**, 555 (1985).
[29] S. Kai, H. Fukunaga, and H. R. Brand, J. Phys. Soc. Jpn. **56**, 3759 (1987).
[30] A. C. Newell and J. A. Whitehead, J. Fluid Mech. **38**, 279 (1969).
[31] A. C. Newell, *Solitons in Mathematics and Physics* (Society for Industrial and Applied Mathematics, Philadelphia, 1985).
[32] M. C. Cross and P. C. Hohenberg, Rev. Mod. Phys. **65**, 851 (1993).
[33] H. R. Brand, P. S. Lomdahl, and A. C. Newell, Phys. Lett. A **118**, 67 (1986); Physica D **23**, 345 (1986).
[34] O. Thual and S. Fauve, J. Phys. (France) **49**, 1829 (1988).
[35] P. Kolodner, D. Bensimon, and C. M. Surko, Phys. Rev. Lett. **60**, 1723 (1988).
[36] J. J. Niemela, G. Ahlers, and D. S. Cannell, Phys. Rev. Lett. **64**, 1365 (1990).
[37] N. Akhmediev and A. Ankiewicz, Editors, *Dissipative Solitons* (Springer, Heidelberg, 2005).
[38] H. R. Brand and R. J. Deissler, Physica A **204**, 87 (1994).
[39] V. B. Taranenko, K. Staliunas, and C. O. Weiss, Phys. Rev. A **56**, 1582 (1997).
[40] G. Slekys, K. Staliunas, and C. O. Weiss, Opt. Commun. **149**, 113 (1998).

[41] E. A. Ultanir, G. I. Stegeman, D. Michaelis, C. H. Lange, and F. Lederer, Phys. Rev. Lett. **90**, 253903 (2003).
[42] P. B. Umbanhowar, F. Melo, and H. L. Swinney, Nature (London) **382**, 793 (1996).
[43] H. H. Rotermund, S. Jakubith, A. von Oertzen, and G. Ertl, Phys. Rev. Lett. **66**, 3083 (1991).
[44] N. Akhmediev and A. Ankiewicz (Eds.), *Dissipative Solitons: From Optics to Biology and Medicine* (Springer, Heidelberg, 2008).
[45] H. R. Brand and R. J. Deissler, Phys. Rev. Lett. **63**, 2801 (1989).
[46] R. J. Deissler and H. R. Brand, Phys. Rev. A **44**, R3411 (1991).
[47] R. J. Deissler and H. R. Brand, Phys. Rev. Lett. **72**, 478 (1994).
[48] V. V. Afanasjev, N. N. Akhmediev, and J. M. Soto-Crespo, Phys. Rev. E **53**, 1931 (1996).
[49] N. Akhmediev, J. M. Soto-Crespo, and G. Town, Phys. Rev. E **63**, 056602 (2001).
[50] S. T. Cundiff, J. M. Soto-Crespo, and N. Akhmediev, Phys. Rev. Lett. **88**, 073903 (2002).
[51] A. F. J. Runge, N. G. R. Broderick, and M. Erkintalo, Optica **2**, 36 (2015).
[52] J. M. Soto-Crespo, N. Akhmediev, and A. Ankiewicz, Phys. Rev. Lett. **85**, 2937 (2000).
[53] O. Descalzi, J. Cisternas, D. Escaff, and H. R. Brand, Phys. Rev. Lett. **102**, 188302 (2009).
[54] C. Cartes, O. Descalzi, and H. R. Brand, Phys. Rev. E **85**, 015205(R) (2012).
[55] O. Descalzi, C. Cartes, and H. R. Brand, Phys. Rev. E **91**, 020901(R) (2015).
[56] O. Descalzi, C. Cartes, and H. R. Brand, Phys. Rev. E **94**, 012219 (2016).
[57] M. Wu, G. Ahlers, and D. S. Cannell, Phys. Rev. Lett. **75**, 1743 (1995).
[58] O. Descalzi, P. Gutierrez, and E. Tirapegui, Int. J. Mod. Phys. C **16**, 1909 (2005).
[59] O. Descalzi and H. R. Brand, Phys. Rev. E **87**, 022915 (2013).
[60] L. Arnold, *Stochastic Differential Equations: Theory and Applications* (Wiley, New York, 1974).
[61] R. Toral and P. Colet, *Stochastic Numerical Methods* (Wiley-VCH, Berlin, 2014).
[62] H. Sakaguchi and H. R. Brand, Physica D **97**, 274 (1996).
[63] P. Kolodner, Phys. Rev. A **44**, 6448 (1991).
[64] P. Kolodner, Phys. Rev. A **44**, 6466 (1991).
[65] A. von Oertzen, A. S. Mikhailov, H. H. Rotermund, and G. Ertl, J. Phys. Chem. B **102**, 4966 (1998).
[66] S.-K. Ma, *Modern Theory of Critical Phenomena* (W. A. Benjamin, Reading, MA, 1976).
[67] G. F. Mazenko, *Fluctuations, Order and Defects* (Wiley, Hoboken, NJ, 2003).
[68] H. Haken, *Synergetics—An Introduction*, 2nd ed. (Springer, Berlin, 1978).
[69] N. Akhmediev and J. M. Soto-Crespo, Phys. Rev. E **70**, 036613 (2004).
[70] J. M. Soto-Crespo, N. Akhmediev, N. Devine, and C. Mejia-Cortes, Opt. Express **16**, 15388 (2008).
[71] O. Descalzi and H. R. Brand, Phys. Rev. E **82**, 026203 (2010).
[72] O. Descalzi, C. Cartes, J. Cisternas, and H. R. Brand, Phys. Rev. E **83**, 056214 (2011).
[73] C. Cartes, J. Cisternas, O. Descalzi, and H. R. Brand, Phys. Rev. Lett. **109**, 178303 (2012).
[74] J. Cisternas, O. Descalzi, T. Albers, and G. Radons, Phys. Rev. Lett. **116**, 203901 (2016).